A RESONANT INVERTER AS A CONTROLLED REACTANCE

Yefim Berkovich[1], Gregory Ivensky[2], and Sam Ben-Yaakov[2*]

[1] Center of Technological Education, Golomb St., 52, Holon 58102, ISRAEL, Tel:+972-3-5026638, Fax: +972-3-5026643, Email: lili_g@barley.cteh.ac.il

[2] Power Electronics Laboratory, Dept. of Electrical and Comp. Engineering, Ben-Gurion Univ. of the Negev, P. O. Box 653, Beer-Sheva 84105, ISRAEL, Tel: +972-7-6461561, Fax: +972-7-6472949, Email: sby@bguee.ee.bgu.ac.il, Web: http:/www.ee.bgu.ac.il/~pel.

Abstract - A new type of a controlled active reactance based on a high frequency resonant inverter with bidirectional switches is proposed and examined. Its important advantages over other approaches are: lower energy stored in reactive elements and lower harmonic distortion.

I. INTRODUCTION

Controlled active reactances applied in active power filters and in static VAR-compensators can be divided into two basic types: those using switch controlled reactors or capacitors [1-3] and those based on inverters in conjunction with energy storage elements (capacitors or inductors) [1-7].

The problems of reducing the stored energy [5,6] and minimizing harmonic distortion [7] in VAR compensators are of great theoretical and practical importance. In this paper we describe a new solution to these problems and examine the potentials of the proposed approach. The essence of the suggested method is the realization of a controlled reactance by a high frequency single phase inverter loaded by a resonant network.

II. TOPOLOGIES

The proposed controlled active reactance can be realized by one of two topologies: applying a parallel resonant network L_rC_r (Fig. 1a) or a series resonant network L_rC_r (Fig. 1b). The resonant circuit is placed in the diagonal of a bridge formed by bidirectional switches S_1-S_4. The other two terminals of the bridge are connected to the ac network of voltage v_o. The interface circuit includes a serially connected filter inductor L_f in the topology of Fig. 1a and a parallel connected filter capacitor C_f in the topology of Fig. 1b. Since the topologies are dual to one another, the paper examines only one of them (Fig. 1a).

III. THEORETICAL ANALYSIS

The commutation function F (Fig. 2) represents the state of switches during a switching period T_S: F=1 when S_1 and S_3 are 'on', F=-1 when S_2 and S_4 are 'on' and F=0 when S_1 and S_2 or S_3 and S_4 are 'on'. The current i_o of the inductor L_f flows into the resonant tank L_rC_r when F=±1 and is shorted via two serially connected switches when F=0. Hence the commutation function F (Fig. 2) has a square waveform with a dead time $t_\alpha=\alpha/\omega_S$ where α is the dead angle in radians and $\omega_S=2\pi/T_S$ is the switching frequency.

The main assumptions of the present analysis are:

1. Ideal switches, capacitors and inductors.
2. The voltage v_o of the ac network does not include high harmonics:

$$v_o = \sqrt{2}V_o \sin(\omega_o t) \qquad (1)$$

where V_o is rms voltage, ω_o is the frequency of the ac network and t is the time.

3. Exact analysis is too cumbersome when $\alpha > 0$ (Fig. 2). Therefore we consider steady state processes taking into account only the first harmonic of the commutation function F:

$$F(1) = \frac{4}{\pi} \cos\alpha \sin(\omega_S t) \qquad (2)$$

When the inverter has a capacitive nature and therefore the first harmonic of its output current $i_{o(1)}$ leads the voltage v_o of ac network (eq. (1)) on $\pi/2$:

$$i_{o(1)} = I_{o(1)m} \cos(\omega_o t) \qquad (3)$$

where $I_{o(1)m}$ is the peak of the first harmonic of the output current. When the inverter has an inductive nature eq. (3) should have a minus sign on the right side.

Applying (2) and (3), the current i feeding the resonant circuit L_rC_r is found to be :

$$i = i_{o(1)}F(1) = \frac{4}{\pi} I_{o(1)m} \cos\alpha \cos(\omega_o t) \sin(\omega_S t) \qquad (4)$$

* Corresponding author

0-7803-5421-4/99/$10.00 © 1999 IEEE

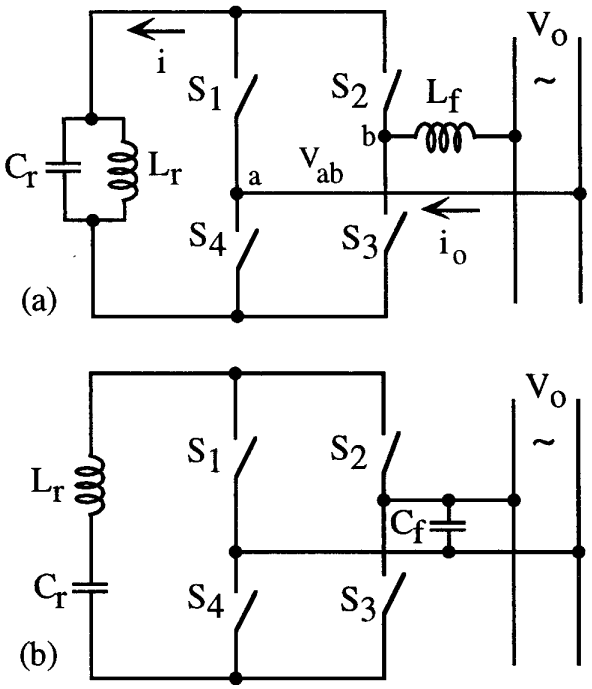

Fig. 1. Proposed controlled active reactances based on resonant inverters: (a) - with parallel resonant network; (b) - with series resonant network. S_1-S_4 are bidirectional switches.

Eq. (4) implies that the current i includes two components with frequencies ω_S-ω_0 and ω_S+ω_0:

$$i = \frac{2}{\pi} I_{o(1)m} \cos\alpha \{\sin[(\omega_S-\omega_0)t] + \sin[(\omega_S-\omega_0)t]\} \quad (5)$$

The voltage v_r across the resonant circuit L_rC_r is found from (5):

$$v_r = -\frac{2}{\pi} I_{o(1)m}\cos\alpha\{X_1\cos[(\omega_S-\omega_0)t]+X_2\cos[(\omega_S-\omega_0)t]\} =$$
$$= -\frac{2}{\pi} I_{o(1)m}\cos\alpha\{(X_1+X_2)\cos(\omega_S t)\cos(\omega_0 t) +$$
$$+ (X_1-X_2)\sin(\omega_S t)\sin(\omega_0 t)\} \quad (6)$$

where X_1 and X_2 are input reactances of the resonant circuit L_rC_r for the frequencies ω_S-ω_0 and ω_S+ω_0:

$$X_1 = \frac{1}{(\omega_S-\omega_0)C_r - \frac{1}{(\omega_S-\omega_0)L_r}} \quad (7)$$

$$X_2 = \frac{1}{(\omega_S+\omega_0)C_r - \frac{1}{(\omega_S+\omega_0)L_r}} \quad (8)$$

The first harmonic of the voltage between the points *a* and *b* (Fig 1a) of the inverter ($v_{ab(1)}$) is found from (6) by replacing the rapidly changing functions $\cos(\omega_S t)$ and $\sin(\omega_S t)$ by their average values during a half period of the switching frequency:

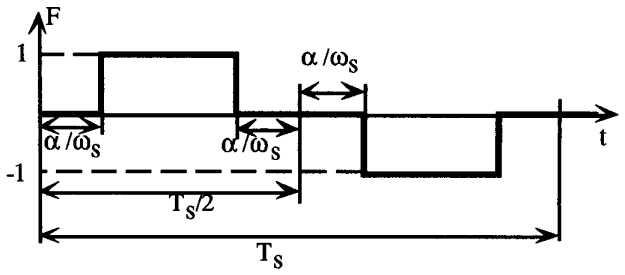

Fig. 2. Waveform of the commutation function F.

$$\frac{1}{\pi}\int_{\alpha}^{\pi-\alpha} \cos(\omega_S t)d(\omega_S t) = 0 \quad (9a)$$

$$\frac{1}{\pi}\int_{\alpha}^{\pi-\alpha} \sin(\omega_S t)d(\omega_S t) = \frac{2}{\pi}\cos\alpha \quad (9b)$$

This approximation is valid under the conditions $\omega_S >> \omega_0$, since the variation of $\cos(\omega_0 t)$ and $\sin(\omega_0 t)$ during a high frequency half period is in this case practically insignificant.

Hence, taking into account (9a) and (9b) we obtain from (6):

$$v_{ab(1)} = V_{ab(1)m}\sin(\omega_0 t) \quad (10)$$

where $V_{ab(1)m}$ is the peak of the first harmonic of this voltage:

$$V_{ab(1)m} = \frac{4}{\pi^2} I_{o(1)m}(X_2-X_1)\cos^2\alpha \quad (11)$$

Applying Kirchhoff's law, the following equation can be written for the case that the inverter exhibits a capacitive nature (Fig. 1a):

$$\sqrt{2}V_o = V_{ab(1)m} - V_{Lf(1)m} \quad (12)$$

where $V_{Lf(1)m}$ is the peak of the first harmonic voltage across the input inductor L_f:

$$V_{Lf(1)m} = I_{o(1)m}\,\omega_0 L_f \quad (13)$$

From (11)-(13) we obtain:

$$I_{o(1)m} = \frac{\sqrt{2}V_o}{X_o} \quad (14)$$

$$V_{ab(1)\,m} = \frac{\sqrt{2}V_o}{1-\frac{\omega_0 L_f}{X}} \quad (15)$$

where X_o is the reactance:

$$X_o = \frac{4}{\pi^2}(X_2-X_1)\cos^2\alpha - \omega_0 L_f \quad (16)$$

and X is the controlled part of the reactance X_o:

$$X = \frac{4}{\pi^2}(X_2-X_1)\cos^2\alpha \quad (17)$$

The inverter has a capacitive nature when:

$$\frac{4}{\pi^2}(X_2-X_1)\cos^2\alpha > \omega_0 L_f \quad (18)$$

and an inductive nature when:

$$\frac{4}{\pi^2}(X_2-X_1)\cos^2\alpha < \omega_0 L_f \quad (19)$$

In the case

$$\frac{4}{\pi^2}(X_2-X_1)\cos^2\alpha = \omega_0 L_f \quad (20)$$

the current fed to the ac network will diverge to infinitely high values exhibiting a unique resonant phenomenon which is linked to the switching action. The nature and frequency of this resonant process differ from the classical resonance of passive networks. Since this phenomenon is due to the switching action, we define it as a "commutator resonance".

The accuracy of the equations derived by above approximate analysis was confirmed by simulation (Fig. 3).The peak current obtained by simulation for the capacitive case (Fig. 3a) is about 6.92A as compared to the calculated value of 6.17A (see parameters in the title of Fig. 3). The peak current obtained by simulation for the inductive case (Fig. 3b) is about 5.38A as compared to the calculated value of 4.74A.

Simulated waveforms of the voltage v_{ab} and of the output current i_o are presented in Fig. 4. The waveforms correspond to the most important case when the inverter operates as a capacitive reactance.

The peak value of the voltage v_{ab} equals to the peak value of the voltage v_r across the resonant link ($V_{ab\ m}=V_{rm}$). This peak is calculated by applying the condition that in the case $\omega_s >> \omega_0$ the value of $v_{ab(1)}$ is practically constant over a half period of the switching frequency, and is therefore equal to the average value of v_{ab} during this half period. Considering the half period which corresponds to $V_{ab(1)m}$ (and hence, to $V_{ab\ m}$) and applying (19b) we find:

$$V_{ab\ m} = V_{rm} = \frac{\pi}{2\cos\alpha} V_{ab(1)m} \quad (21)$$

or taking into account (15)

$$V_{ab\ m} = V_{rm} = \frac{\pi}{2\cos\alpha} \frac{\sqrt{2}V_0}{1-\frac{\omega_0 L_f}{X}} \quad (22)$$

The rms voltage across the resonant network is half its peak value (because the high frequency carrier is modulated by the low frequency component of the ac network) :

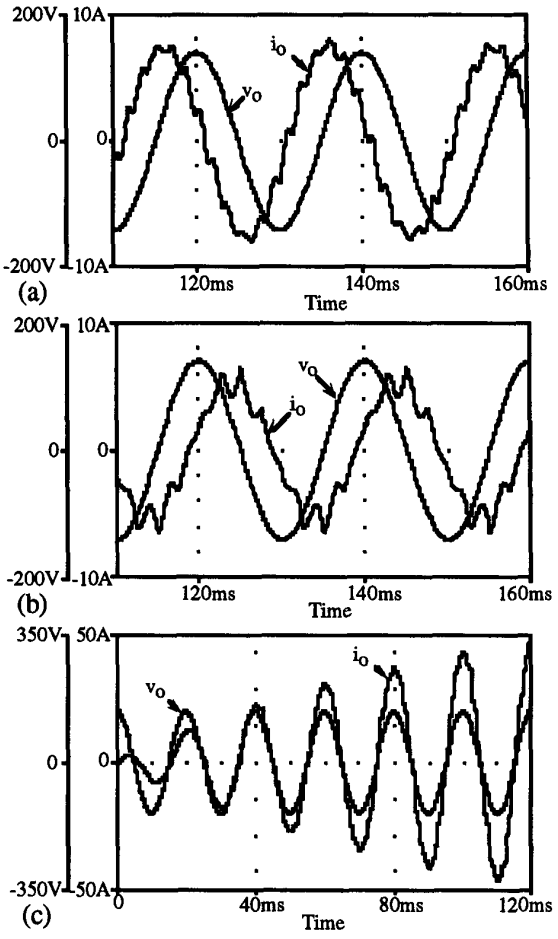

Fig. 3. Simulated current i_o transferred to an ac network of voltage v_o by proposed inverter under various operating conditions: (a) - capacitive reactance; (b) - inductive reactance; (c) - commutator resonance.
V_o=100 V, L_r=7.18 mH, C_r=42 μF, ω_0=314 rad/sec, α=0; In (a): L_f=50 mH, ω_s=1963.5 rad/sec. In (b): L_f=50 mH, ω_s=1256.6 rad/sec. In (c): L_f=100 mH, ω_s= 1885 rad/sec.

$$V_{r\ rms} = \frac{\pi}{4\cos\alpha} \frac{\sqrt{2}V_0}{1-\frac{\omega_0 L_f}{X}} \quad (23)$$

Average energy stored in the electric field of the capacitor C_r and in the magnetic field of the inductor L_r is found from (23):

$$E_{Cr} = E_{Lr} = \frac{C_r V_{r\ rms}^2}{2} = \frac{\pi^2}{16} \frac{C_r V_0^2}{\cos^2\alpha} \frac{1}{(1-\frac{\omega_0 L_f}{X})^2} \quad (24)$$

Analysis shows that in addition to the first harmonic the voltage v_{ab} includes harmonics of the order

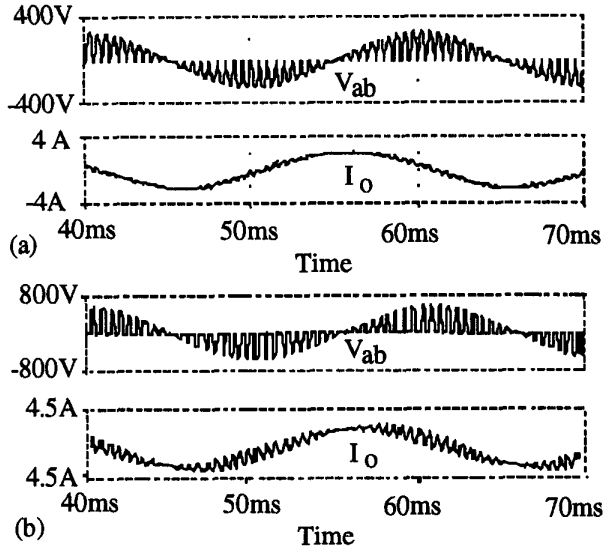

Fig. 4. Simulated voltage v_{ab} and current i_o waveforms: V_o=100 V, L_f=40 mH, ω_o=314 rad/sec, ω_s=6280 rad/sec. Upper two traces: α=0, L_r=1.6 mH, C_r=16 μF. Lower two traces $\alpha=\frac{\pi}{3}$, L_r=16 mH, C_r=4 μF.

$$h = 2\,g\,k_s \pm 1 \tag{25}$$

where k_s is the frequency ratio

$$k_s = \frac{\omega_s}{\omega_o} \tag{26}$$

and g=1,2,3, ... ,∞. Thus, if the switching frequency ω_s is much higher than the frequency of the ac network ω_o, low order harmonics will not be injected into the ac network. For example, if k_s=20 the lowest harmonics order (after the first) will be 39, 41, 79, 81.

The peaks of h-order harmonics are expressed by following equation (for α=0):

$$V_{ab(h)m} = \frac{2}{\pi}\frac{V_{ab\,m}}{4g^2-1} \tag{27}$$

IV. Comparison to Other Types of Controlled Reactances

The following discussion is for the case when the uncontrolled part $\omega_o L_f$ of the reactance X_o (eq. (26)) is considerably smaller than the controlled part X:

$$\omega_o L_f << X \tag{28}$$

In this case, the output current of the inverter i_o (i.e. the current of the controlled capacitive reactance) is mainly determined by the reactance X. It is also assumed that the switching frequency ω_s is close to the resonant frequency of the ideal L_rC_r network and is much higher than the frequency ω_o of the ac network:

$$\omega_s \approx \frac{1}{\sqrt{L_rC_r}} >> \omega_o \tag{29}$$

Under these conditions (27) can be transformed to:

$$X = \frac{4}{\pi^2}\sqrt{\frac{L_r}{C_r}}\,k_s\cos^2\alpha \tag{30}$$

The last equation expresses the reactance X as a function of the actual L_r, C_r elements and can therefore be used as a basis for comparing the proposed approach to other methods.

For example, in the controlled reactance topology of Fig. 5a, a capacitor C_o is connected in parallel to a switch-controlled reactor L_o [1,5]. Hence, C_o (Fig. 5a) replaces the reactance X at ω_o. Taking into account this requirement and applying (26), (29), (30), the following approximated relationship is obtained:

$$C_o = \frac{\pi^2}{4\cos^2\alpha}C_r \tag{31}$$

The switch controlled reactor L_o must compensate (when needed) the current of C_o. Therefore, its inductance can be found from the trivial expression:

$$L_o = \frac{1}{\omega_o^2 C_o} \tag{32}$$

Applying (26), (29) and (31) we obtain:

$$L_o = \frac{4k_s^2\cos^2\alpha}{\pi^2}L_r \tag{33}$$

Average energy stored in the electric field of the capacitor C_o and in the magnetic field of the inductor L_o is calculated from (31):

$$E_{Co} = E_{Lo} = \frac{C_oV_o^2}{2} = \frac{\pi^2}{8}\frac{C_rV_o^2}{\cos^2\alpha} \tag{34}$$

Comparison of (34) to (24) reveals that the energy stored in the reactive elements C_o and L_o (Fig. 5a) is approximately twice higher than in the proposed controlled reactance (Fig. 1a).

Comparison to controlled reactances topologies that apply non-resonant inverters and a large capacitance (or large inductance) as a DC energy storage (Figs. 5b and 5c) was carried out in a similar way.

Approximate relationships between the energy stored in the capacitor of the voltage-fed non-resonant inverter $E_{Cn\text{-}r}$ (Fig. 5b) and in the capacitor of the proposed controlled reactance E_{Cr} (Fig. 1a) are dependent on the operating mode of the non-resonant inverter:

without PWM

$$\frac{E_{Cn\text{-}r}}{E_{Cr}} = \frac{\pi}{2\Delta V_C^*} \quad (35)$$

when operating in PWM mode

$$\frac{E_{Cn\text{-}r}}{E_{Cr}} = \frac{2}{\Delta V_C^*} \quad (36)$$

where ΔV_C^* is the relative ripple (ripple voltage divided by DC component) of the DC voltage across the capacitor of the voltage-fed non-resonant inverter. The energy stored in the inductances of the inverter (Fig. 5b) is negligible small whereas in the proposed resonant inverter (Fig. 1a) the energy is equal E_{Cr}. Taking in account this consideration and assuming that ΔV_C^* is limited to 10%, we find from (35) and (36) that the total energy of the reactive elements of the non-resonant voltage-fed inverter operating without PWM is approximately eight times higher than in the proposed resonant inverter and is ten times higher when the non-resonant inverter operates in PWM mode.

Topologies of voltage-fed and current-fed non-resonant inverters (Figs. 5b and 5c) are dual to one another and therefore the total energy stored in reactive elements of both inverters is the same. For the current-fed inverter case (Fig. 5c), (35) and (36) need to be transformed to the dual configuration:

without PWM

$$\frac{E_{Ln\text{-}r}}{E_{Lr}} = \frac{\pi}{2\Delta I_L^*} \quad (37)$$

when operating in PWM mode

$$\frac{E_{Ln\text{-}r}}{E_{Lr}} = \frac{2}{\Delta I_L^*} \quad (38)$$

where $E_{Ln\text{-}r}$ is the energy stored in the inductor of the current-fed non-resonant inverter (Fig. 5c), E_{Lr} is the energy stored in the inductor L_r of the proposed controlled reactance (Fig. 1a) and ΔI_L^* is the relative ripple (ripple current divided by DC current) of the DC current of the inductor L in the current-fed non-resonant inverter.

The harmonic components injected into the ac network by the proposed resonant inverter are lower in comparison to other approaches including those operating in the PWM mode in which the switching frequency is much higher than the line frequency and when a special technique for minimization of law order harmonics is used [7].

V. Discussion and Conclusions

The proposed variable inductance can be realized by one of two possible approaches: with zero α or with variable α.

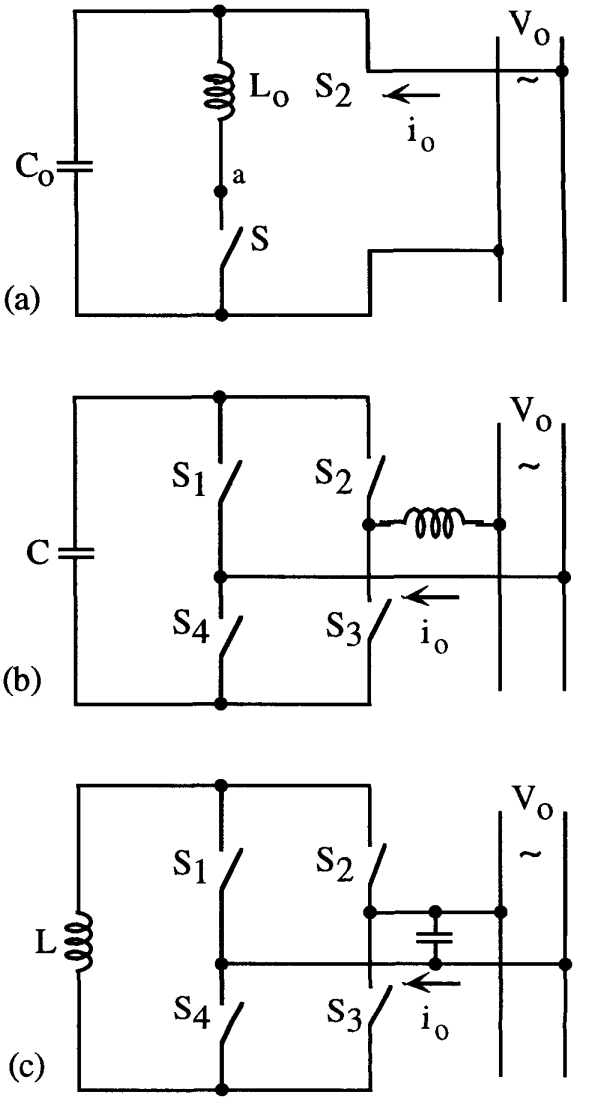

Fig. 5. Earlier proposed controlled reactances [1-7]: (a) - with a switch controlled inductor L_o, S-bidirectional switch; (b) - non-resonant voltage-fed inverter, S_1-S_4 - uni-directional switches with anti-parallel diodes; (c) - non-resonant current-fed inverter, S_1-S_4 - uni-directional switches without anti-parallel diodes.

The main differences between the two approaches are:

1. The zero α case calls for variable switching frequency but provide Zero Voltage Switching (ZVS) of the inverter.
2. In the non zero case, switching frequency can be constant but commutation is in hard switching mode.

The conclusions of this study are summarized as follows:

1. A resonant inverter applying bidirectional switches and loaded by a resonant tank can be used to emulate a capacitive or inductive reactance. The magnitude of the reactance can be controlled by changing the switching frequency or by

applying PWM. An apparent resonant phenomenon, "commutator resonance", is discovered and its dependence on the topology elements and operating conditions is derived. This resonance process differs from known resonant conditions in electrical networks that do not include switches.

2. When the switching frequency of the resonant inverter is much higher than the frequency of the ac network, the proposed inverter is useful as a VAR-compensator. Hence, this inverter is a new addition to known families of VAR-compensators which are based on voltage-fed and current-fed non-resonant inverters. The advantages of the new topology are: lower energy stored in reactive elements and lower injection of harmonics into the ac network. Harmonic distortion is greatly reduced when the switching frequency is much higher than the ac line frequency.

3. Approximate design equations for the proposed variable reactance were derived. Their validity was confirmed by simulation.

REFERENCES

[1] L. Gyugyi, "Power electronics in electric utilities: static VAR compensators", *Proceedings of the IEEE*, v. 76, no. 4, 1988, pp. 483-494.

[2] J. D. van Wyk, "Power quality, power electronics and control", *Proceedings EPE'93*, Brighton, pp. 17-32.

[3] D. A. N. Jacobson and R. W. Menzies, "Comparison of thyristor switch capacitor and voltage source GTO inverter type compensators for single phase feeders", *IEEE Transactions on Power Delivery*, v. 7, no. 2, 1992, pp. 776-781.

[4] H. Funato, A. Kavamura, K. Kamiyama, "Realization of negative inductance using variable active-passive reactance (VAPAR)", *IEEE Transactions on Power Electronics*, v. 12, no. 4, 1997, pp. 589-597.

[5] J. He and N. Mohan, "Switch-mode VAR compensator with minimized switching losses and energy storage elements", *IEEE Transactions on Power Systems*, v. 5, no.1, 1990, pp. 90-95.

[6] Ch.-Y. Hsu and H.-Y. Wu, "A new single-phase active power filter with reduced energy storage capacitor", *Proceedings PESC'95*, pp. 202-208.

[7] Z. Chen and S. B. Tennakoon, "A technique for the reduction of harmonic distortion and power losses in advanced static VAR compensators", *Proceedings APEC'95*, pp. 620-626.